Enhanced weak-signal sensitivity in two-photon microscopy by adaptive illumination

Kengyeh K. Chu, Daryl Lim, and Jerome Mertz*

Department of Biomedical Engineering, Boston University, 44 Cummington Street, Boston, Massachusetts 02215, USA
**Corresponding author: jmertz@bu.edu*

Received May 16, 2007; accepted August 30, 2007;
posted September 4, 2007 (Doc. ID 83115); published September 26, 2007

We describe a technique to enhance both the weak-signal relative sensitivity and the dynamic range of a laser scanning optical microscope. The technique is based on maintaining a fixed detection power by fast feedback control of the illumination power, thereby transferring high measurement resolution to weak signals while virtually eliminating the possibility of image saturation. We analyze and demonstrate the benefits of adaptive illumination in two-photon fluorescence microscopy. © 2007 Optical Society of America

OCIS codes: 110.0180, 180.2520, 180.5810, 190.4180.

Scanning fluorescence microscopy techniques such as confocal [1] and two-photon [2] microscopy have become mainstream research tools. In their conventional implementations a laser beam of constant intensity is scanned through a sample, and the resulting fluorescence signal from the sample is measured by a detector and assigned to a pixel location to form an image. The gamut of detectable levels is typically defined by the dynamic range, the highest measurable value before saturation divided by the smallest detectable difference.

Dynamic range in biological imaging is frequently challenged by the diversity of image levels within the sample. If the dynamic range is insufficient to capture this diversity, then the brightest areas of the image are saturated or the nuances of the faint structures are lost. We report in this Letter a method of overcoming the dynamic range limitation by departing from the standard paradigm of using constant illumination. We instead use a negative feedback loop to hold the average detected power at a constant level by controlling the power of the illumination beam with an analog modulator. We refer to this technique as adaptive illumination (AI).

Our paradigm of constant versus variable detection is well known from nonoptical scanning microscopy technologies in which the dynamic range of the desired measurable is the limiting factor, such as scanning tunneling microscopy or atomic force microscopy [3]. Recently a similar technique called controlled light exposure microscopy (CLEM) has been applied in the optical domain [4]. CLEM operates by shutting off the laser power once the prescribed amount of signal light has been detected from a given pixel. AI microscopy differs in that the laser power can be modulated over the entire range between completely off and full power. While the main purpose of CLEM is to minimize exposure of the sample to unnecessary illumination, leading to reduced photobleaching, the goal of AI microscopy is instead to improve sensitivity and signal-to-noise performance for weakly fluorescent objects.

The layout of an AI microscope is shown in Fig. 1. An electro-optic modulator (EOM, Conoptics 350-80) outputs laser power P, which interacts with the sample. Signal power S from the sample is detected (Electron Tubes PC125-05 photomultiplier), and the voltage output of the detector is compared with a set point value V_{set} (corresponding to a set point signal power S_{set}) to produce an error signal. A proportional-integral-derivative (PID) feedback circuit then acts to minimize this error by producing a correction signal that acts upon the EOM, completing the loop. A voltage limiter also sets a maximum voltage V_{max} (corresponding to a maximum illumination power P_{max}) used in the attempt to reach the set point to avoid photodamage [5].

We implemented this method in two-photon fluorescence (TPEF) imaging (laser: Amplitude Système t-pulse at 1030 nm). In conventional TPEF, the detection power S is recorded using a constant illumination power P_0. The measurable parameter of interest X, here proportional to the fluorophore concentration, is derived then from the simple relation $S=P_0^2X/\alpha$, where α is a constant accounting for unit conversions and detector gain. That is, S is the dynamic quantity that carries the sample information.

In AI-TPEF, both S and P are recorded. The target parameter X is again simply recovered by

$$X=\frac{\alpha S}{P^2}. \tag{1}$$

However, in this case S is subject to feedback control. We identify two feedback regimes: in the ideal case where the feedback properly holds S to its set point, $S\rightarrow S_{set}$ and the dynamic quantity that carries the sample information in Eq. (1) is transferred to P. We call this the feedback active (FA) regime. However, because P is limited to a maximum value P_{max}, the

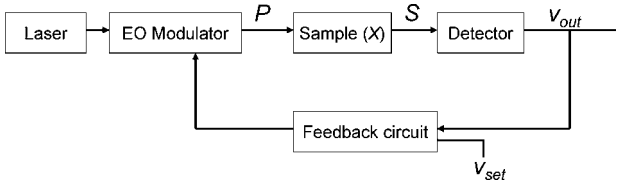

Fig. 1. AI microscope layout. Signal power S from a sample X is detected, producing a voltage V_{out} that is maintained at a set point V_{set} by analog feedback to an EOM that controls the illumination power P.

set point cannot be attained when X is too small. In this case, $P \rightarrow P_{max}$ and the dynamic quantity that carries the sample information reverts to S. We call this the power-limited (PL) regime.

We define the relative sensitivity of an imaging system as the derivative of the desired parameter X with respect to the measured quantity S or P for fixed power or fixed signal regimes, respectively. In this definition, a smaller relative sensitivity is better, since this indicates a smaller resolvable step in X for an equal step in S or P. In the FA regime, the relative sensitivity is

$$\Sigma_{FA} = \frac{1}{X}\frac{\partial X}{\partial P} = 2\sqrt{\frac{X}{\alpha S_{set}}}, \quad (2)$$

and in the PL regime it is

$$\Sigma_{PL} = \frac{1}{X}\frac{\partial X}{\partial S} = \frac{\alpha}{P_{max}^2 X}. \quad (3)$$

We compare these relative sensitivities to that of conventional TPEF, which is defined by Eq. (3) but with P_{max} replaced by P_0. Several conclusions can be drawn from a plot of these relative sensitivities, shown in Fig. 2. First, because S is held approximately constant in the FA regime, the relative sensitivity of AI-TPEF is skewed to the lower range of X relative to that of conventional TPEF. However, the very smallest values of X cannot fall under this regime since illumination power that exceeds P_{max} would be required. AI-TPEF then switches to the PL regime. From Eq. (3) the relative sensitivity in this regime is still improved over that of conventional TPEF provided P_{max} is greater than P_0. We emphasize that setting P_{max} to a greater value than P_0 does not necessarily imply that the total power delivered to the sample is greater in AI-TPEF than in conventional TPEF, but only that it is greater in sample regions that are weakly flourescent. Also, high illumination powers are not constrained by the risk of out-of-focus photobleaching when using two-photon excitation, obviating the need to suppress excitation in regions of very weak fluorescence [4].

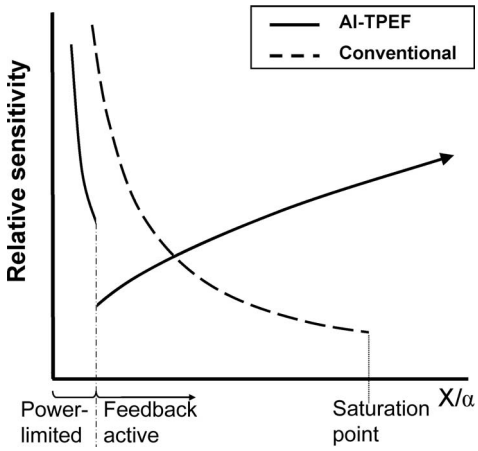

Fig. 2. Relative sensitivity dependence on fluorophore concentration (lower is better). The dashed curve represents conventional TPEF microscopy; the discontinuity at the right indicates saturation. The solid curve denotes AI-TPEF microscopy; the discontinuity towards the left occurs when the illumination power reaches maximum and the system crosses into the PL regime. $P_{max} > P_0$ in this plot.

At the opposite end of the dynamic range, using conventional microscopy (i.e., constant power), high X values require lower P or lower amplifier gain (manifested as decreased α) to prevent saturation. The trade-off is diminished sensitivity in the lower register of X: to image the higher intensities, the ability to resolve small changes in small signals becomes sacrificed. This is the standard limitation imposed by dynamic range.

In contrast, saturation is virtually eliminated when using AI. The feedback circuit employs low P values when confronted with high X to maintain the set point. Because P can be reduced arbitrarily close to zero (limited only by EOM contrast), added to the fact that the P dependence of X is quadratic for TPEF, an effectively infinite range of X can be imaged. The cost of this infinite range is decreased sensitivity in the upper register of X. The ability to see small changes in smaller signals comes at the expense of detecting small changes in large signals. This is not an unreasonable sacrifice given that saturation in conventional microscopy prevents any sort of quantification of the upper range. The point at which conventional detection and AIM share the same relative sensitivity is found by finding the intersection of Σ_{FA} and Σ_{PL}. For X/α values below this point, AI-TPEF has the sensitivity advantage. Above it, conventional TPEF is superior, until saturation is reached, at which point only AI-TPEF provides any sensitivity at all.

The images in Fig. 3 illustrate the capabilities of AI-TPEF microscopy. The brighter points in Fig. 3a are held to a constant set point. Figure 3b represents the power used to attain the set point value in Fig. 3a. The white background in this image is our prescribed maximum power P_{max}; pixels that are white are therefore in the PL regime. Figure 3(c) shows the X reconstruction based on the previous two images. This reconstruction appears similar to the conventional TPEF image (Fig. 3d); however, a closer inspection shown in Figs. 3e and 3f illustrates the improved AI-TPEF signal-to-noise ratio (SNR) for a dim area of the sample.

In the AI-TPEF images, the parameters were set such that P_{max} was slightly greater than the power P_0 used for the conventional TPEF image, but the set point S_{set} was low enough that the total fluorescence power recovered from the cell was actually lower for the AI-TPEF image (same integration times for both). This setting represents a balance between improved relative sensitivity at low intensities (where more power is used in AI-TPEF) and sacrificed relative sensitivity at high intensities (where less power is used in AI-TPEF).

Shot noise is also altered by the introduction of feedback in AI microscopy. In the FA regime the rate of photons incident on the detector is held relatively constant over the duration of a pixel acquisition. SNR

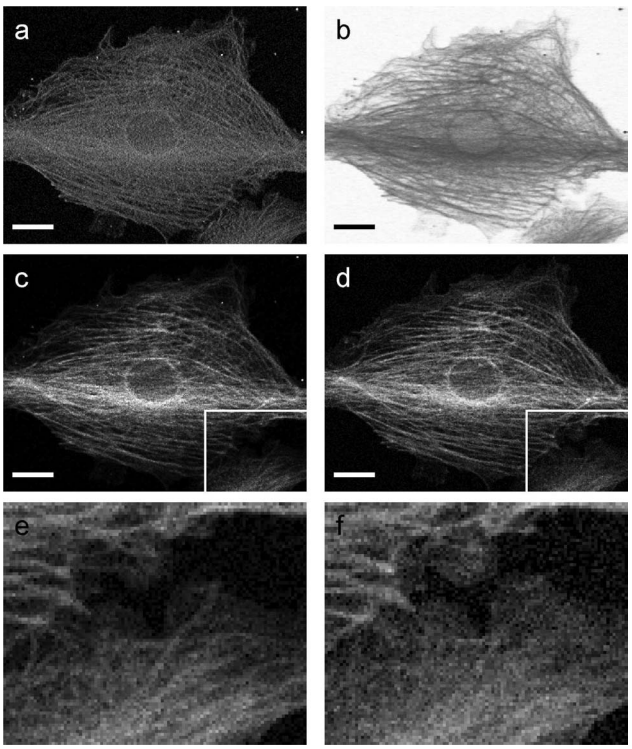

Fig. 3. AI-TPEF image reconstruction of prepared bovine pulmonary artery endothelial (BPAE) cells, actin labeled with Texas Red-X phalloidin. Scale bar 20 μm. a, Image of S (12-bit), held by the feedback circuit to a set point. b, Image of P (12-bit), output of the feedback circuit to the EOM, corresponding to the illumination power used. c, Reconstructed X image (float). d, Conventional TPEF image (12 bit). e and f, Enlargements of the insets from c and d, respectively, both with applied gamma correction of 0.65.

due to shot noise therefore scales as $\sqrt{S}$. Because S is raised via feedback to equal or approach S_{set}, shot noise SNR performance is improved for lower signal levels and is constant for FA pixels. Alternatively, in the PL regime the shot noise contribution is no longer constant, but because the illumination power in this regime is typically greater than that used in conventional imaging (i.e., $P_{\max} > P_0$), shot noise related SNR is still improved, as shown in Figs. 3e and 3f.

In Fig. 4, the range advantage of AI microscopy is manifest. A cell containing an anomalously bright body was imaged by both conventional and AI-TPEF, and the corresponding X images are presented on a logarithmic brightness scale. The bright body is saturated in conventional TPEF but not AI-TPEF, while at the same time the SNR and relative sensitivity at the dimmer regions of the sample are superior for AI-TPEF. To achieve the same SNR in conventional TPEF would have required more illumination power, provoking even more saturation, or alternatively less detector gain, provoking a potentially greater influence of detector fluctuations, amplifier noise, or digitization error. Figure 4(c) compares the two images on a histogram. Conventional TPEF leads to marked saturation, while AI-TPEF is able to quantify much higher values. The zoomed-in inset demonstrates better AI-TPEF bit resolution as a result of improved relative sensitivity and redistributed dynamic range; the AI-TPEF image is much less discretized in the lower register than the conventional image. We note that to obtain Figs. 3 and 4 our microscope was operated at its standard pixel acquisition rate of 125 kHz. Our feedback bandwidth was larger than this, about 1 MHz, meaning that the application of AI in no way impaired the standard image acquisition rate of our microscope.

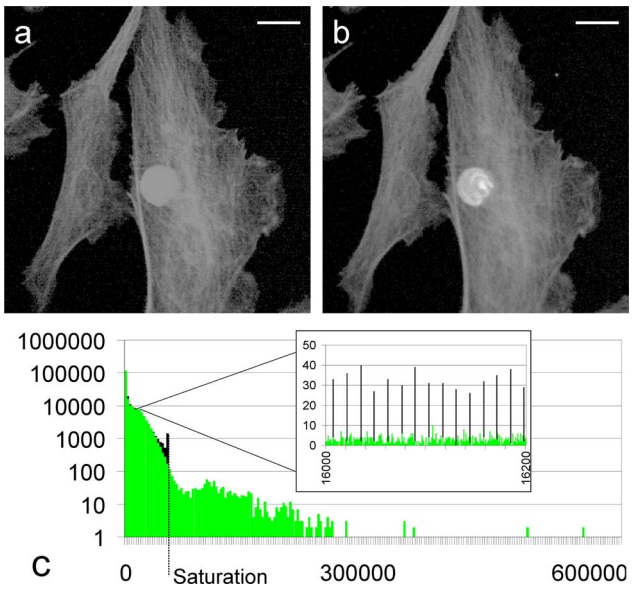

Fig. 4. (Color online) Logarithmic gray-scale map of Invitrogen Fluocells 2 fibroblast images. Scale bar 20 μm. a, Conventional TPEF image (12-bit). b, AI-TPEF reconstructed image (float). Images a and b are normalized to the same maximum pixel value. c, Histograms of images a (black) and b (green or gray) on a log y-axis. Inset, zoomed-in portion of the histogram with a linear y-axis.

We conclude that adaptive illumination is useful in TPEF microscopy and indeed in any scanning imaging technique in which saturation and SNR at low intensities are limiting factors, such as samples with both bright objects and dim objects. AI microscopy enhances the ability to see small changes in small signals while at the same time providing an effectively infinite imaging range. Because of its simplicity and ease of implementation, we anticipate that AI microscopy will be useful to the bioimaging community.

References

1. J. B. Pawley, *Handbook of Biological Confocal Microscopy* (Springer, 2006).
2. W. Denk, J. H. Strickler, and W. W. Webb, Science **248**, 73 (1990).
3. E. Meyer, H. J. Hug, and R. Bennewitz, *Scanning Probe Microscopy: the Lab on a Tip* (Springer, 2003).
4. R. A. Hoebe, C. H. Van Oven, T. W. J. Gadella Jr., P. B. Dhonukshe, C. J. F. Van Noorden, and E. M. M. Manders, Nat. Biotechnol. **25**, 249 (2007).
5. G. H. Patterson and D. W. Piston, Biophys. J. **78**, 2159 (2000).